

Supplementary Material - Methods

S.1. Sonoma County geography information and Soundscapes 2 Landscapes site stratification: forest chemistry and structure

Seasonal average precipitation in Sonoma County is 247 mm in spring [March – May], 9 mm in summer [June – August], 185 mm in fall [September – November], and 600 mm in winter [December – February] (NOAA, 1981–2010 U.S. Climate Normals: Ground stations in the county). Natural vegetation in Sonoma County includes evergreen conifer (Coastal redwoods [*Sequoia sempervirens*], Douglas fir [*Pseudotsuga menziesii*]) and broadleaf forests (Tan oak [*Notholithocarpus densiflorus*], Coast live oak [*Quercus agrifolia*]) in western coastal mountains, as well as mixed forests of deciduous (Black oak [*Quercus kelloggii*], Oregon white oak [*Quercus garryana*], California buckeye [*Aesculus californica*]) and evergreen broadleaf trees (Coast live oak), conifers (Douglas fir) and shrubs.

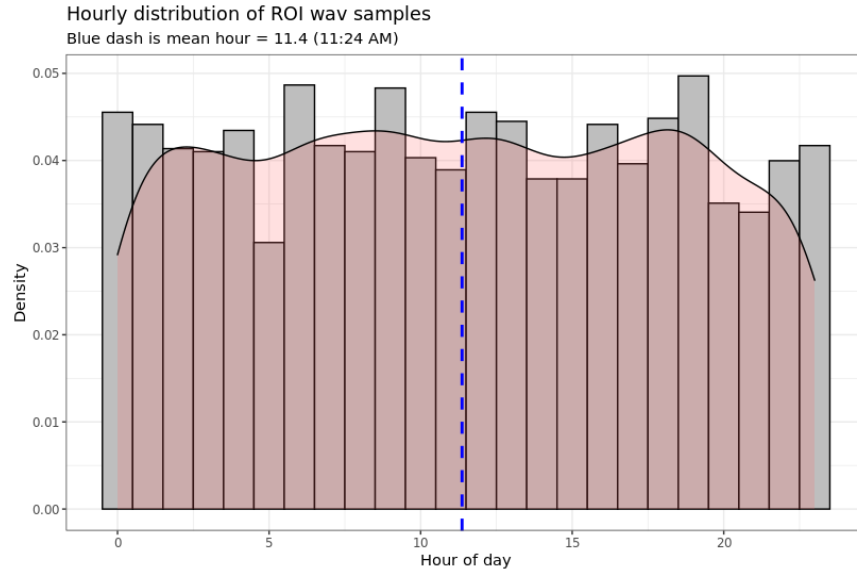
We used stratified random sampling to identify locations for ARUs across Sonoma County. The geographic information systems (GIS) software ArcGIS Pro software was used to create strata based on county-wide GIS data (i.e., terrain, streams, land cover), canopy chemistry (i.e., chlorophyll, nitrogen, lignin, water) metrics from summer 2017 airborne hyperspectral imagery (Clark & Kilham, 2016), and forest structure metrics (derived using LAStools) from 2013 airborne lidar. We first stratified the county into upland and lowland zones using a digital elevation model. A county land-cover map (<http://sonomavegmap.org/data-downloads/>) was used to separate annual croplands, developed areas, grasslands, native forests, orchards, shrublands, vineyards, urban-wildland, and other areas. Further, riparian corridors were delineated as 25-m from lidar-derived streams. Forests were separated into six chemical and structural variation levels based on principal component analysis applied to multi-seasonal hyperspectral and lidar metrics, respectively. Many of these random sample points fell in inaccessible terrain (e.g., in a ravine or atop a steep hill); therefore, when deploying ARUs, citizen scientists chose a subset of the random sample points on each property based on navigation feasibility. When no stratified sample points fell on the property (usually due to small property size), or when none of the sample points were accessible, we defined a set of parameters for the citizen scientist to use to select a site on the property: (1) away from the road and house, (2) >50 meters from any bird feeders on the property, (3) feasible to navigate to, and (4) use no a priori knowledge regarding bird activity.

S.2. Sampling effort – LULC by-year count of S2L sites

Table S.2.1
Count of LULC sites by year

Year	Urban/ Developed	Agriculture/ Barren	Herbaceous	Shrubland	Riparian/ Wetland	Oak/Hardwood Forest	Conifer Forest	Total
2017	2	4	15	8	0	63	30	122
2018	0	0	20	6	6	30	27	89
2019	10	3	78	25	15	111	103	345
2020	3	4	34	8	0	79	62	190
Total	15	11	147	47	21	283	222	746

S.3. ROI recording file sampling distribution by the hour of the day



S.4. Regions of interest sound class composition

Table S.4.1

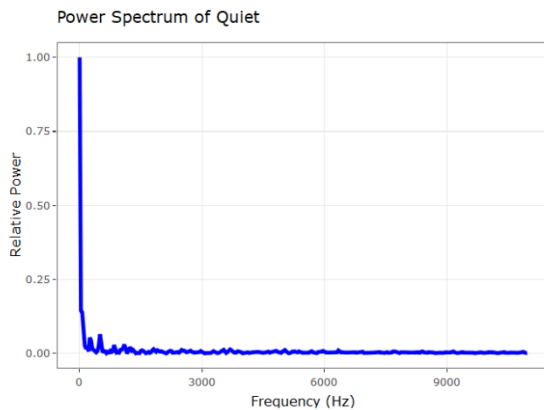
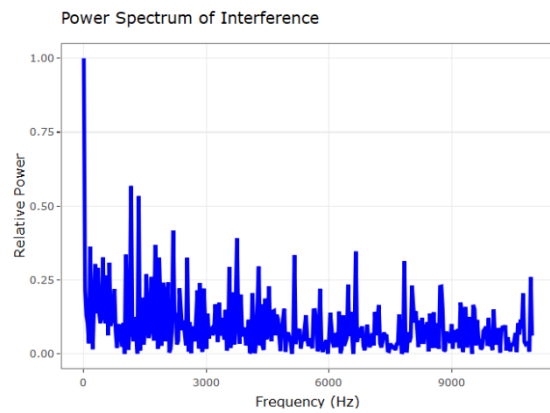
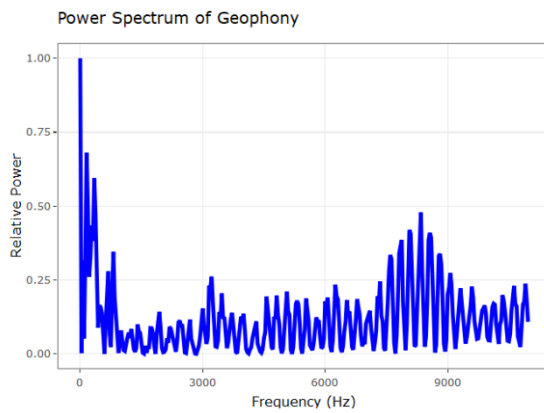
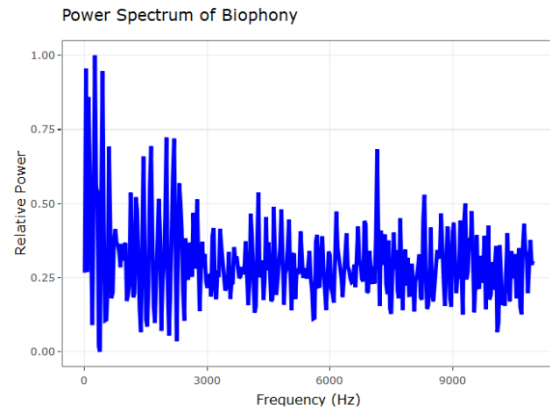
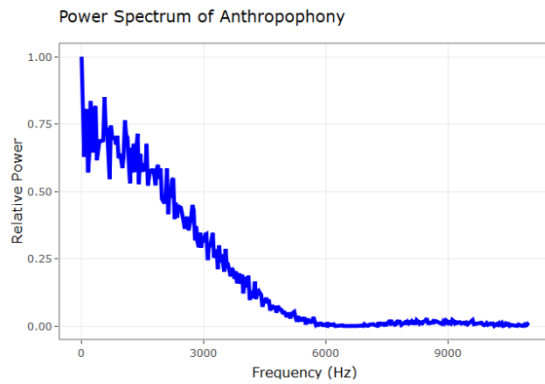
Target soundscape classes and specific sounds that compose each class are used to annotate regions of interest. Total spectrogram samples, including Freesound, are noted in parentheses.

Sound Class	Included sounds
Anthropophony	Air traffic (n = 398), vehicle horn (n = 53), vehicle traffic (n = 828), rail traffic (n = 23), siren (n = 17), machinery (e.g., generators, chain saws; n = 781), human voice (n = 70)
Biophony	Birds (n = 1,745), insects (n = 667), amphibians (n = 778), mammals (n = 146)
Geophony	Rain (n = 415), wind – constant (n = 484), wind – gust (n = 432), stream (n = 589), ocean (n = 35)
Quiet	Little to no perceptible noise, i.e., background (n = 1,023)
Interference	Broad frequency physical or electronic recording disturbance (n = 430)

S.5. Sound class normalized spectral power characteristics – power and frequency

Power spectral density plots display power along the frequency domain used for the CNN (0-11 kHz). They were calculated using the discrete fast Fourier transform (Dfft) from the package fftw (version 1.0-5) and a 32-ms window from which power was derived using $\frac{|Dfft|^2}{n \text{ samples}}$. This calculation was done on a single, concatenated .wav file containing all 2-s ROI segments for each model class. These plots demonstrate the frequency regions with high and low levels of power. To note, quiet contains a majority of its signal power in low-frequency regions (<500 Hz) primarily due to the inherent noise from the recording device. Comparatively, other sound classes vary in power along with the frequency range. Anthropophony has high power at low frequencies, fading to minimal power above 6 kHz. Biophony shows the recorder activity at low frequency and then a range of activity through

higher frequencies. Geophony displays most of its power below 1 kHz with a 7-9 kHz spike. Interference has a consistent amount of power long the frequency range reflecting its characteristic broadband frequency signature.



S.6. ROI identification and Mel Spectrogram generation methods

Mel Spectrogram creation

The 2-s Mel spectrograms were created using Python’s librosa library, version 0.6.3, using an HTK implementation with the following parameters: max frequency = 11,025 Hz, sampling rate = 22,050, fast Fourier transfer window = 728, 32 samples per frame (a temporal resolution control), and 128 Mels displayed on the linear frequency scale (converting the power spectrogram to decibel (dB) units).

Freesound event detection and segmentation

Freesound filenames are provided in the project Zenodo repositories. Each Freesound file was listened to for quality by C.Q. (i.e., was the intended sound present) and relative clarity (i.e., was the intended signal identifiable or mixed significantly with other signals). We identified potential ROIs with R version 4.0.2 through RStudio version 1.3.1093 using autototec function in warbleR package (Araya-Salas ad Smith-Vidaurre, 2017), which provided start and stop times of possible ROIs. We used start and end times of events to generate Mel spectrograms in Python, following the same methods as S2L ROI segmentation.

S.7. Augmentation experiment

We applied a single augmentation, shifting the pitch of samples using librosa.effects.pitch_shift. The pitch was offset using a random value from a Gaussian normal distribution (mean = 0, sd = 0.25) (Lasseck 2019). These data were included in only the training data split – increasing the dataset from 7,814 to 15,628 samples (augmented files were not included from the validation or test datasets). Accuracy was higher with augmentation using the same CNN architecture, S2L bird vocalization pretraining, and Freesound data (F0.75 score increase of 0.070).

Table S.7.1
Evaluation metrics from test data following recording augmentation

	Precision	Recall	F0.75-score
Anthropophony	1.000	0.880	0.961
Biophony	0.939	0.920	0.929
Geophony	0.978	0.880	0.926
Quiet	0.960	0.960	0.960
Interference	0.980	0.980	0.980
Avg.	0.970	0.924	0.953

However, because our spectrogram generation and test dataset code were not adapted for augmentation of the dataset following training, the training dataset includes augmented spectrograms of all the non-augmented testing data. This may positively bias our testing metrics. To provide an independent assessment of how augmentation influences model performance, we used the soundscape validation dataset (S.12) to compare with the non-augmented performance (ABGQI-CNN). We did not utilize augmentation at this time because soundscape validation performance was only marginally improved at the cost of a doubling in training computation time. However, other augmentation, especially mixed signals or multilabel data, could improve performance and is worth further investigation.

Table S.7.2

Evaluation metrics derived from the soundscape-validation dataset following recording augmentation

	Precision	Recall	F1-score
Anthropophony	0.564	0.562	0.563
Biophony	0.937	0.827	0.879
Geophony	0.670	0.691	0.680
Interference	0.682	0.905	0.778

S.8. S2L bird ROI data for MobileNetv2 pre-training

The Soundscapes to Landscapes project has amassed ~750,000 minutes of data (4.3 Terabytes), from which we needed citizen scientists (CS) to help collect sample clips of bird calls and songs for training deep learning bird classification models. We used the web-based Arbimon platform to facilitate this work, allowing users to sort, visualize, listen to, and identify bird vocalizations from sound recordings (Aide et al., 2013). We partnered with Sieve Analytics (the platform’s creator) to design a custom C.S. interface for bird call/song reference data collection.

In the Arbimon CS interface, a volunteer with bird-call identification knowledge (i.e., “expert”) delineates a bounding box representing a single bird call or song within a 1-minute spectrogram. The system then uses this template region of interest (ROI) and a pattern matching algorithm (LeBien et al. 2020) to find similar ROIs above a specified correlation threshold in our extensive collection of sound recordings. This results in hundreds to thousands of potential matches. The expert experimented with the template used and the correlation threshold to provide as many present ROI matches as possible for C.S. review while minimizing the number of clips where the bird was absent. Experts generally varied the threshold by species (minimum=0.075, maximum=0.45, average=0.29) with up to 10 matches per recording and up to 500 matches per site between 5 a.m. to 7 p.m. for diurnal species and 8 p.m. to 6 a.m. for nocturnal species.

The Arbimon CS interface allows user- and expert-level C.S. to quickly validate if matched ROIs include the bird call or song found in the template ROI. Using the template ROI as a reference, the user-level C.S. can validate a given matched ROI by assessing the visual spectrogram pattern or by listening to the sound clip, a process that needs minimal training and requires no a priori knowledge of bird calls. The system records validations of the same ROI among multiple user-level C.S. and provides a consensus vote. We chose a threshold of three user-level C.S. votes for either present or absent to reach a consensus, and matched ROIs had a maximum of five votes before a given ROI entered a validated set and was removed from further review. The expert C.S. can view statistics for all C.S. to compare their relative accuracy and make adjustments, such as improving training to reduce errors. Additionally, expert C.S. can provide sole votes on ROIs to quickly boost the number of present ROIs in the reference data, and they can also review consensus validations to reduce false presences. This approach allowed our C.S. to develop large numbers of reference ROI data for 54 species of birds with 178,160 absences and 51,906 presences.

S.9. ABGQI-CNN training

The ABGQI-CNN was trained in two stages: (1) model training on the classifier only (i.e., dense, fully-connected layer), freezing all other trainable parameters for 10 epochs (learning rate = 0.0001), and (2) fine-tuning the network by freezing layers 1-50 and adjusting the final 105 layers for 10 more epochs. See GitHub code repository for code used to fine-tune the pre-trained MobileNetV2 CNN

(1_fine-tune_ABGQI-CNN.ipynb). Model weights were saved only when the internal validation loss decreased.

S.10. Soundscape modeling, multivariate regression methods

We began with a full model that included all candidate variables, quadratic and cubic distance to road, interactions between LULC with road distance, and interaction between sound type with road distance. We also generated a model containing only soundType acting as the simplest model we explored. Below are our calls to the linear modeling command in R and a table explaining each covariate and the response. If a description includes a count (n), this represents a categorical variable. We included nonlinear terms represented with a caret (^) and interactions between two covariates represented with (*). Model fit was evaluated using MASS::stepAIC, with forward and backward selection starting with the full model. At each step, model fit was evaluated, and the covariate with the lowest AIC, which may give less information to the model, is eliminated, and the model is refit and reevaluated iteratively.

Table S.10.1

Description of response and covariates for the linear regression modeling

Response	Description
logitRate	Logit value of the rate of positively predicted 2-s samples at the site. Positively predicted 2-s samples are the count of samples predicted positive. The rate of positive predicted samples is calculated as $\frac{positive}{total\ samples}$. Each site (n = 746) then had five observations/rows, one for each soundType.

Covariate	Description
LULC	Land use land cover classes (n = 7).
logRoadDist	The natural logarithm of the distance to the nearest road from the observation.
Year	The year recordings took place (n = 4).
Log(Number_of_spectrograms)	The log of the number of total 2-s spectrograms at the site. A measure of sampling effort.
soundType	The class of sound (n = 5). Each sound was modeled as an offset in this model.
Recorder	ARU model (n = 2).
DOY	The day of initial field deployment. A measure of seasonality.

Full model (AIC = 13702.69):

```
lm(formula = logitRate ~ LULC + I(logRoadDist^2) + I(logRoadDist^3) + Year +
  log(number_mel_spectrograms) + soundType + Recorder + DOY + LULC*logRoadDist +
  soundType:logRoadDist)
```

Simple model (AIC = 13769.80):
`lm(formula = logitRate ~ soundType)`

Final model (AIC = 13687.75):
`lm(formula = logitRate ~ LULC + Year + log(number_mel_spectrograms) + soundType + logRoadDist + soundType:logRoadDist)`

S.11. Cross-validation F(β) threshold results

In the optimal cross-validation iteration F0.75-score model, there were 15.6% unidentified test ROIs, which decreased to 9.2% with the optimal F1-score model. However, this improvement in the F1-score model reducing unidentified samples came at the cost of 0.033 overall lower precision. Change in average precision was similar from the F0.50-score model (0.968 ± 0.032) to the F0.75-score model (0.936 ± 0.038); however, average recall was low for the F0.50-score model (0.760 ± 0.100) compared to the F0.75-score model (0.804 ± 0.055) coupled with 21.6% unidentified data in the optimal F0.50-score model. F0.75-score decreased the amount of unidentified sound relative to F0.50-score while decreasing false positives compared to the F1-score thresholds. Increasing the F(β)-score in threshold optimization resulted in lower threshold values (i.e., more liberal classification of positive predictions) and higher false-positive rates.

Table S.11.1

Cross-validation model performance for F(β) threshold values based on withheld test data for each sound class.

F(β) threshold	Precision	Recall	F0.75-score	F1-score
0.50	0.940 ± 0.02	0.698 ± 0.04	0.829 ± 0.03	0.795 ± 0.03
0.75	0.902 ± 0.03	0.754 ± 0.03	0.838 ± 0.03	0.817 ± 0.03
1.00	0.844 ± 0.04	0.815 ± 0.04	0.829 ± 0.03	0.825 ± 0.03

S.12. Soundscape-validation: an independent assessment of accuracy

For soundscape validation, we randomly sampled recordings from the entire S2L dataset based on a stratification determined by time and acoustic indices (Salas 2020). First, a suite of acoustic indices was calculated: Acoustic Complexity Index, Acoustic Evenness Index, Acoustic Diversity Index, Normalised Difference Soundscape Index, Acoustic Entropy Index, Temporal Entropy (Sueur et al. 2014), and Bioacoustic Index (Boelman et al. 2007). We first split recordings by time of day: dawn (6 a.m. to 9 a.m.), mid-day (11 a.m. to 2 p.m.), and late afternoon (4 p.m. to 7 p.m.). We then applied a K-mean clustering to acoustic indices to produce clusters within each period. We chose the number of clusters by examining the drop of the within-cluster mean sum of squared errors (MSE) and selected a number that represented the point where the MSE reached an asymptotic value from which adding clusters minimally decreased the within-cluster MSE. In all three time periods, the number of clusters chosen was 6. We sampled 50 recordings per cluster, yielding 900 GV samples for review, of which 710 were reviewed.

The 710 recordings were listened to for the presence and absence of anthropophony, biophony, geophony, and interference at the 1-min level. At the review, quiet was not established as a modeling class and is omitted here. We compared reviewed recordings to 2-s spectrogram ABGQI-CNN

predictions aggregated to the 1-min level (presence and absence) and generated confusion matrix classification evaluation metrics. We expect these evaluation metrics to be lower than the test dataset metrics as this test reflects the accuracy of our applied analyses while test metrics reflect model accuracy. We observe high accuracy for biophony and interference and lower accuracy for anthropophony and geophony.

Table S.12.1
Soundscape validation accuracy at the 1-min recording level.

	True Pos.	False Pos.	False Neg.	True Neg.	Precision	Recall	F1-score
Anthropophony	131	108	72	396	0.548	0.645	0.593
Biophony	437	35	101	134	0.926	0.812	0.865
Geophony	204	118	116	269	0.634	0.638	0.636
Interference	287	110	30	280	0.723	0.905	0.804

S.13. Summary of soundscape classes in a random sample of unidentified samples

We randomly selected 60 recordings with significant unidentified predictions (1-min recordings with greater than the median number of 2-s samples with unidentified) and included a summary of what soundscape classes author C.Q. heard during each 2-s unidentified sample (n = 832).

The most significant samples remained unidentifiable due to static, distant ambiguous low-frequency noise or masking by other sounds. Anthropophony was the next most commonly unidentified and included sounds we did not have in the ROI training set (i.e., talking, digital beeping) or were faint that may not display in the Mel spectrograms (distant traffic or plane). This latter point was also the case with biophony and geophony. A significant number of samples with biophony were extremely faint and may not have resolved in the 2-s Mel spectrograms. Other prominent issues included a persistent electronic buzz in recordings between 7-10 kHz that may have masked other sounds. Co-occurring, mixed classes appear to have been missed in some cases, though at a lower rate than the faint signals or ambiguous noises described above.

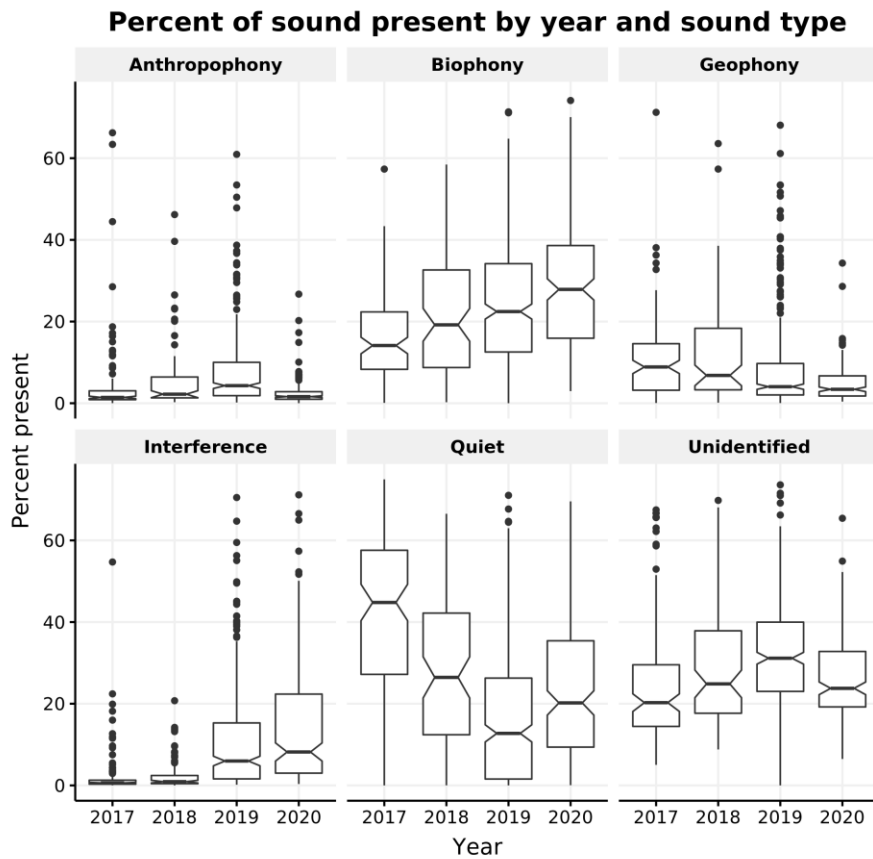
Table S.13.1
Percent of sound types that co-occur during 2-s unidentified samples from CNN

Sounds	Count	Percent
Unknown noise	129	15.5%
Anthropophony (A)	113	13.6%
Quiet (Q)	81	9.75%
Biophony (B)	76	9.15%
Geophony (G)	72	8.7%
B + I	70	8.4%

B + G	70	8.4%
Interference (I)	63	7.6%
A + B	60	7.2%
A + I	28	3.4%
A + B + I	20	2.4%
G + I	22	2.7%
B + G + I	19	2.3%
A + G	6	0.7%
A + G + I	1	0.1%
A + B + G	1	0.1%

S.14. Amount of sound stratified by year

The amount of sound for each sound type is shown below, grouped by site.



S.15. Pairwise test statistic summary tables

Table S.15.1

Sample counts for paired test groups—number of sites per LULC.

LULC	n
Urban/Developed	15
Agriculture/Barren	11
Herbaceous	147
Shrubland	47
Riparian/Wetland	21
Oak/Hardwood Forest	283
Conifer Forest	221

Section 3.2.1: Diurnal LULC patterns

Table S.15.2

Mann-Whitney's U tests reveal significant differences in the amount of day and night sound. Significant tests in bold ($p < 0.05$).

Soundscape class	U	p-value
Anthropophony	2.364x10⁷	0.0000
Biophony	1.917x10⁷	0.0000
Geophony	3.464x10⁷	0.0000
Quiet	5.032x10⁷	0.0000
Interference	3.161x10⁷	0.0000
Unidentified	3.556x10⁷	0.0000

Section 3.2.2: Annual and date of deployment differences

Table S.15.3

The number of sites (sample counts) for non-overlapping and overlapping deployment dates by year. Overlapping date range: May-01 to July-05

Year	Non-overlapping n	Overlapping n
2017	122	65
2018	89	46
2019	345	193
2020	190	156

Table S.15.4

Kruskal-Wallis analysis testing significant differences in the amount of sound among years when subset to overlapping deployment dates (May-01 to July-05). Significant tests in bold ($p < 0.05$).

Soundscape class	Chi-square (χ^2)	p-value
Anthropophony	35.049	1.19x10⁷
Biophony	29.582	1.69x10⁶
Quiet	75.744	2.51x10¹⁶

Table S.15.5

Dunn analyses testing significant differences of annual sound for overlapping deployment dates (May-01 to July-05). Significant pairs in bold ($p\text{-adj} < 0.05$).

Soundscape class	Year pair	z value	p-adj value
Anthropophony	2017-2018	0.4824	1.0000
	2017-2019	3.4100	0.003898
	2017-2020	-0.8233	1.0000
	2018-2019	2.4139	0.09469
	2018-2020	-1.2785	1.0000
	2019-2020	-5.6710	8.516x10⁸
Biophony	2017-2018	1.9850	0.2829
	2017-2019	4.6692	1.814x10⁵
	2017-2020	5.0657	2.442x10⁶
	2018-2019	1.7501	0.4806

	2018-2020	2.1778	0.1765
	2019-2020	0.7267	1.0000
Quiet	2017-2018	-1.0886	1.0000
	2017-2019	-7.7693	4.737x10¹⁴
	2017-2020	-5.3004	6.932x10⁷
	2018-2019	-5.5123	2.124x10⁷
	2018-2020	-3.4138	0.003843
	2019-2020	3.0806	0.01240

Section 3.2.3: Daytime LULC stratification

Table S.15.6

Kruskal-Wallis analysis testing significant differences of LULC daytime sound. Significant tests in bold ($p < 0.05$).

Soundscape class	Chi-square (χ^2)	p-value
Anthropophony	97.798	0.0000
Biophony	18.891	0.004351
Geophony	4.8538	0.5627
Quiet	109.92	0.0000

Table S.15.7

Dunn analyses testing significant differences of LULC daytime sound for significant Kruskal-Wallis tests. Significant pairs in bold ($p\text{-adj} < 0.05$).

Soundscape class	LULC pair	z value	p-adj value
Anthropophony	Urban/Developed - Agriculture/Barren	-1.0425	1.0000
	Urban/Developed - Herbaceous	-3.1630	0.03279
	Urban/Developed - Shrubland	-4.5056	0.0001390
	Urban/Developed - Riparian/Wetland	-0.9831	1.0000
	Urban/Developed - Oak/Hardwood Forest	-4.9930	1.249x10⁵
	Urban/Developed - Conifer Forest	-5.9314	6.310x10⁸

	Agriculture/Barren - Herbaceous	-1.4188	1.0000
	Agriculture/Barren - Shrubland	-2.7537	0.1238
	Agriculture/Barren - Riparian/Wetland	0.2190	1.0000
	Agriculture/Barren - Oak/Hardwood Forest	-2.9581	0.06501
	Agriculture/Barren - Conifer Forest	-3.7830	0.003255
	Herbaceous - Shrubland	-2.8575	0.08968
	Herbaceous - Riparian/Wetland	2.2504	0.5129
	Herbaceous - Oak/Hardwood Forest	-4.5794	9.793x10⁵
	Herbaceous - Conifer Forest	-6.8184	1.934x10¹⁰
	Shrubland - Riparian/Wetland	3.8243	0.002754
	Shrubland - Oak/Hardwood Forest	0.08411	1.0000
	Shrubland - Conifer Forest	-1.5333	1.0000
	Riparian/Wetland - Oak/Hardwood Forest	-4.3797	0.0002495
	Riparian/Wetland - Conifer Forest	-5.4752	9.177x10⁷
	Oak/Hardwood Forest - Conifer Forest	-2.8939	0.07989
Biophony	Urban/Developed - Agriculture/Barren	-1.7355	1.0000
	Urban/Developed - Herbaceous	-1.1698	1.0000
	Urban/Developed - Shrubland	-0.8144	1.0000
	Urban/Developed - Riparian/Wetland	0.3717	1.0000
	Urban/Developed - Oak/Hardwood Forest	-0.0170	1.0000
	Urban/Developed - Conifer Forest	-1.0343	1.0000
	Agriculture/Barren - Herbaceous	1.1896	1.0000
	Agriculture/Barren - Shrubland	1.3358	1.0000
	Agriculture/Barren - Riparian/Wetland	2.1886	0.6012
	Agriculture/Barren - Oak/Hardwood Forest	2.2271	0.5447
	Agriculture/Barren - Conifer Forest	1.3370	1.0000
	Herbaceous - Shrubland	0.4510	1.0000
	Herbaceous - Riparian/Wetland	1.8978	1.0000

	Herbaceous - Oak/Hardwood Forest	3.0745	0.04428
	Herbaceous - Conifer Forest	0.3869	1.0000
	Shrubland - Riparian/Wetland	1.3988	1.0000
	Shrubland - Oak/Hardwood Forest	3.0745	1.0000
	Shrubland - Conifer Forest	-0.2145	1.0000
	Riparian/Wetland - Oak/Hardwood Forest	-0.5754	1.0000
	Riparian/Wetland - Conifer Forest	-1.7590	1.0000
	Oak/Hardwood Forest - Conifer Forest	-3.0275	0.05178
Quiet	Urban/Developed - Agriculture/Barren	0.7280	1.0000
	Urban/Developed - Herbaceous	2.0062	0.9414
	Urban/Developed - Shrubland	4.6819	5.968x10⁵
	Urban/Developed - Riparian/Wetland	-0.4612	1.0000
	Urban/Developed - Oak/Hardwood Forest	4.5876	9.414x10⁵
	Urban/Developed - Conifer Forest	4.5724	0.0001013
	Agriculture/Barren - Herbaceous	0.8152	1.0000
	Agriculture/Barren - Shrubland	3.2825	0.02161
	Agriculture/Barren - Riparian/Wetland	-1.1953	1.0000
	Agriculture/Barren - Oak/Hardwood Forest	3.0149	0.05398
	Agriculture/Barren - Conifer Forest	3.0135	0.05424
	Herbaceous - Shrubland	5.0405	9.751x10⁶
	Herbaceous - Riparian/Wetland	-2.9994	0.05681
	Herbaceous - Oak/Hardwood Forest	6.6068	8.244x10¹⁰
	Herbaceous - Conifer Forest	6.3573	4.311x10⁹
	Shrubland - Riparian/Wetland	-5.8836	8.428x10⁸
	Shrubland - Oak/Hardwood Forest	-1.0979	1.0000
	Shrubland - Conifer Forest	-1.0502	1.0000
	Riparian/Wetland - Oak/Hardwood Forest	6.0636	2.795x10⁸

Riparian/Wetland - Conifer Forest	6.0258	3.534x10⁸
Oak/Hardwood Forest - Conifer Forest	0.0480	1.0000

Section 3.2.4: Distance to roads

Table S.15.8

Sample counts for paired test groups—the number of sites in road distance classes.

Road distance classes	n
0-99m	184
100-199m	131
200-299m	94
300-399m	68
400-499m	64
500-599m	44
600-699m	21
700-799m	25
800-899m	25
900-999m	20
> 1000m	70

Table S.15.9

Kruskal-Wallis analysis tested significant distance differences to road groups (100m) daytime sound. Significant tests in bold ($p < 0.05$).

Soundscape class	Chi-square (χ^2)	p-value
Anthropophony	48.543	4.939x10⁷
Biophony	16.5	0.08618
Geophony	18.139	0.05267
Quiet	46.521	1.154x10⁶

Table S.15.10

Dunn analyses testing significant differences of annual sound for significant Kruskal Wallis tests. Only significant pairs are shown and are bold (p-adj < 0.05). All values can be derived from 1_KWDunn_tests-LULC_Roads_DateofDeploy.R in the code repository.

Soundscape class	Road pair	z value	p-adj value
Anthropophony	0-99m & 400-499m	-3.9048	0.005186
	0-99m & >1000m	-5.0636	2.263x10⁵
	100-199m & 400-499m	-3.7069	0.01154
	100-199m & >1000m	-4.7939	8.997x10⁵
Quiet	0-99m & 900-999m	3.7253	0.01073
	0-99m & >1000m	4.7566	0.0001083
	100-199m & >1000m	3.8575	0.006300

S.16. Computational efficiency

The ABGQI-CNN took 4 hours to train on a laptop with an NVIDIA Quadro M1200 GPU and 16 G.B. of RAM, and approximately 100 collective hours of ROI dataset generation. Inference was a function of the S2L dataset size and took approximately 250 hours of computing time, but was calculated on multiple computing nodes taking only 6 hours to complete. The model can be trained and deployed on a dataset similar to the S2L dataset in a single day with a small, labeled dataset. We estimate inference can be done on a single CPU with 2GB RAM at a rate of 200, 1-min recordings (each represented by 30, 2-s spectrograms) per hour.

S.17. ABGQI-CNN relative performance

Table S.17.1

Comparison of soundscape-component classification across select studies implementing CNN image classification or other methods. These include select studies from the environmental sound classification (ESC) field. We have used precision (Prec.) and recall (Rec.) as these metrics were most common in studies; other metrics reported when precision and recall were unavailable. nRMSE = normalized root mean square error; Acc. = n correct predictions / n incorrect predictions.

Study	Classification Method	Anthropophony	Biophony	Geophony
Quinn et al. (2022)	ABGQI-CNN with transfer learning and pre-training (5 classes)	Prec.=0.975	Prec.=0.913	Prec.=0.923
This study.		Rec.=0.780	Rec.=0.840	Rec.=0.720
		Acc.=0.952	Acc.=0.952	Acc.=0.932
Fairbrass et al. (2019)	Custom CNNs for Anthro- and Biophony (2, 1 class CNNs)	Prec.=0.977	Prec.=0.934	NA
		Rec.=0.858	Rec.=0.710	NA

Mullet et al. (2016)	Stochastic gradient boosting regression and spatial modeling (3 classes)	nRMSE=21%	nRMSE=20%	nRMSE=20%
Salamon and Bello (2017)	Custom CNN with data augmentation (10 classes)	Acc.=0.803±0.125	NA	NA
Piczak (2015)	Custom CNN using multiple soundscape datasets and augmentation	Acc.(ESC.50)=0.645, Acc.(UrbanSound8K)=0.737	NA	NA
Inik and Seker (2020) Table 3 summarizes ESC accuracies	Grid-search of CNN parameters classifying UrbanSounds8k (10 classes)	Acc.=0.8245	NA	NA

References

- Aide TM, Corrada-Bravo C, Campos-Cerqueira M, Milan C, Vega G, Alvarez R. Real-time bioacoustics monitoring and automated species identification. *PeerJ*. 2013 Jul 16;1:e103. doi: <https://doi.org/10.7717/peerj.103>
- Araya-Salas M, Smith-Vidaurre G (2017). “warbleR: an r package to streamline analysis of animal acoustic signals.” <https://dx.doi.org/10.1111/2041-210X.12624>.
- Clark, M. L., & Kilham, N. E. (2016). Mapping of land cover in northern California with simulated hyperspectral satellite imagery. *ISPRS Journal of Photogrammetry and Remote Sensing*, 119, 228-245.
- Lasseck, M., 2019. Bird species identification in soundscapes. *CEUR Workshop Proc.* 2380.
- LAStools, “Efficient LiDAR Processing Software”, obtained from <http://rapidlasso.com/LAStools>
- LeBien J, Zhong M, Campos-Cerqueira M, Velez JP, Dodhia R, Ferres JL, Aide TM. A pipeline for identification of bird and frog species in tropical soundscape recordings using a convolutional neural network. *Ecological Informatics*. 2020 Sep 1;59:101113. doi: <https://doi.org/10.1016/j.ecoinf.2020.101113>
- Salas, L., 2020. soundscapeIndicesOrdination.R. Available at *GitHub Repository*, <https://github.com/pointblue/s2lcitsci>